BPR MCS | Bulletin of Pioneering Researches of Medical and Clinical Science

**Bulletin of Pioneering Researches of Medical and Clinical Science**

**Available online:** https://bprmcs.com
**2024 | Volume 4 | Issue 2 | Page: 167-176**

# Characterization of a Cytotoxic Transglutaminase from Mycobacterium spp. Driving RIPK1 Activation

**Claire Martin[1], Julien Robert[2]*, Sophie Bernard[1], Antoine Girard[2]**

[1]Department of Clinical and Biomedical Sciences, University of Lyon, Lyon, France.
[2]Department of Medical Research Innovation, University of Strasbourg, Strasbourg, France.

## Abstract

Although worldwide tuberculosis case rates have dropped in the last few years, the disease persists as an immense challenge to global public health. The *Mycobacterium tuberculosis* complex (MTBC), comprising *M. tuberculosis*, *M. bovis*, and *M. microti*, among others, stands as the most lethal *Mycobacterium* spp. warranting intensified scrutiny. Research focused on *M. microti* is particularly important given its status as a zoonotic pathogen capable of moving between animal reservoirs and people. By probing the role of a transglutaminase enzyme in *M. microti* (MmTG), which is broadly present across *Mycobacterium* and other organisms, a putative cytotoxic effector has been delineated. MmTG blocks cellular multiplication through the induction of RIPK1 (receptor-interacting serine/threonine-protein kinase 1) phosphorylation, and the Cys159 position of MmTG represents the highly conserved residue tied to its toxic activity. Deciphering MmTG and its homologs can yield a deeper understanding of mycobacterial disease mechanisms and support the design of more efficacious treatment options for mycobacterial infections.

**Keywords:** *Mycobacterium* spp, MmTG, RIPK1, Cytotoxicity, Transglutaminase

**Corresponding author:** Julien Robert
**E-mail:** julien.robert@gmail.com

**How to Cite This Article:** Martin C, Robert J, Bernard S, Girard A. Characterization of a Cytotoxic Transglutaminase from Mycobacterium spp. Driving RIPK1 Activation. Bull Pioneer Res Med Clin Sci. 2024;4(2):167-76. https://doi.org/10.51847/CGQOBHS5ci

## Introduction

Ranking among the most consequential communicable illnesses, tuberculosis (TB) remains a pressing public health worry, disproportionately affecting low- and middle-income settings. In 2023, 8.2 million newly diagnosed TB cases were documented worldwide, a tally that shows ongoing growth compared with earlier periods. Achieving the objective of a TB-free world remains a distant ambition [1]. The *Mycobacterium tuberculosis* complex (MTBC) encompasses a collection of closely related mycobacteria, notably *M. tuberculosis*, *M. bovis*, *M. microti*, and other species [2], all capable of infecting a wide array of hosts and primarily causing tuberculosis of variable intensity in diverse mammals. Due to the varied pathogenic strategies employed by the MTBC, its potent immune evasion skills, substantial genetic plasticity, and the intricacy of acquired antimicrobial resistance [3, 4], the processes of clinical detection and therapeutic management of TB are laden with hurdles. These realities not only hinder patient care but also impose serious economic pressures on affected individuals and their households.

TB, caused by *M. tuberculosis*, primarily spreads through the airborne route. Even though it principally appears as a pulmonary disease, it can also disseminate to multiple organs and tissues, generating extrapulmonary conditions such as osseous tuberculosis and other localized or widespread TB forms [5]. In parallel, *M. bovis*, the chief etiological agent of bovine tuberculosis, is likewise considered to be associated with human pathology. People

may acquire *M. bovis* through direct exposure to livestock or by ingesting unpasteurized dairy products or insufficiently cooked meat. Such occurrences are notably frequent in certain developing regions [6]. Consequently, to safeguard human health and advance TB control, it is imperative to look beyond human-restricted pathogens and meaningfully limit the spread of animal-residing microorganisms, which can directly shape the burden of human tuberculosis. Tuberculosis was first observed in voles in 1948 and later classified as *M. microti*, which was subsequently acknowledged within the MTBC [7]. While it predominantly affects voles, it has also shown a broad host spectrum, demonstrating pathogenic potential in species including goats, badgers, wild boars, and dogs, as well as humans [8, 9]. As a zoonotic pathogen, *M. microti* multiplies slowly in the laboratory and possesses biochemical properties that are not readily distinguishable from those of other MTBC members. In addition, the molecular underpinnings of its capacity to cause human illness remain insufficiently elucidated, thus creating major obstacles for clinical recognition and medical intervention [10].

Transglutaminase (TGase) is an enzyme that drives acyl-transfer chemistry and can be categorized by source into animal-origin TGases, plant-origin TGases, and microbial transglutaminases (mTGs) [11, 12]. Animal-origin TGases have been extensively explored, notably transglutaminase 2 (TG2), which is widely expressed and functionally versatile. TG2 occupies critical positions in the regulation of gene activity, signaling cascades, immune function, and inflammatory responses. It engages in varied cellular activities, including transamidation, serving as a Gα signal transducer, a protein disulfide isomerase (PDI), a protein kinase, and a structural scaffold. Within the nucleus, it chemically modifies histones and transcriptional regulators [13]. In contrast, the biological contributions of mTGs within the MTBC remain poorly defined. TGases may play important roles in mycobacterial virulence, potentially acting as toxic effectors, and they share a conserved Cys-His-Asp motif within the core catalytic center [14, 15]. The Photorhabdus virulence cassette (PVC), a contractile injection apparatus that functions outside the cell, contains a needle-like architecture that translocates effector proteins (e.g., toxins) into host cells [16], thereby providing a powerful means to investigate bacterial cytotoxicity. Our group has previously applied the PVC system to characterize the function of candidate bacterial toxins and to examine their engagement with host cells [17].

In the present work, we characterized a gene, annotated as PLV44373.1, in *Mycobacterium tuberculosis* variant microti OV254 (*M. microti* transglutaminase, MmTG), which encodes a transglutaminase. Through transient overexpression, PVC-assisted protein translocation into J774A.1 cells, and macrophage infection assays, we measured the toxic properties and identified a conserved catalytic residue of MmTG. Computational sequence analysis revealed that TGase is widely distributed and highly conserved across mycobacterial lineages. Moreover, the corresponding homolog in *M. abscessus* shows cytotoxicity against eukaryotic cells and stimulates RIPK1 phosphorylation. This study helps identify candidate mycobacterial toxins and offers fresh perspectives on their pathogenic strategies.

## Materials and Methods

### *Bacterial handling and mammalian cell cultivation*

#### *Bacterial growth conditions*

Liquid LB medium at 37 °C was used to propagate all E. coli variants. DNA cloning and plasmid amplification were performed in E. coli DH5α, whereas the EPI300 strain was reserved exclusively for the preparation of PVC particles. *Mycobacterium smegmatis* mc2155 and the corresponding recombinant line, Ms_Vec, were maintained in Middlebrook 7H9 broth at 37 °C with orbital shaking at 220 rpm. Where required, the following selective agents were introduced at the specified working strengths: ampicillin at 100 μg/mL, tetracycline at 10 μg/mL, kanamycin at 25 μg/mL, gentamycin at 20 μg/mL, and chloramphenicol at 25 μg/mL.

#### *Eukaryotic cell line maintenance*

Both the J774A.1 murine macrophage-like line and the HEK293T human embryonic kidney line were kept in Dulbecco's Modified Eagle Medium (DMEM, Thermo Fisher Scientific, New York, NY, USA, C11995500BT) formulation containing 10% fetal bovine serum (FBS, Thermo Fisher Scientific, A5669701) alongside 1×Penicillin–Streptomycin (MedChemExpress, New Jersey, NJ, USA, 100 μg/mL streptomycin and 100 U/mL penicillin, HY-K1006). The THP-1 line, derived from human monocytic leukemia, was cultivated in RPMI 1640 base medium (Thermo Fisher Scientific, C11875500BT) identically enriched with 10% FBS and the same antibiotic cocktail. Incubation conditions for all cultures were a humidified 37 °C chamber with 5% CO2.

### *Construct assembly and genetic engineering*

Within the scope of this work, transient eukaryotic MmTG production relied on the pEGFP-C1 vector; heterologous MmTG expression in M. smegmatis used pMV261; and pBBRN-pdp1N50 served as the delivery vector for PVC cargo protein fusions. Two additional elements were co-deployed to orchestrate the formation of intact PVC particles: the multi-gene construct pRK404-PVC, which carries the 16 structural components of the PVC apparatus, and pBR322-LysR. This companion plasmid supplies the regulatory factors indispensable for correct supramolecular assembly. The gene segment encoding

MmTG was chemically synthesized with a design that placed, at its 5′ terminus, the forward homology region corresponding to pMV261 together with a BamHI recognition sequence, while its 3′ end featured the reverse homology region matching pMV261, a HindIII recognition motif, and a tail encoding six consecutive histidine residues. For overexpression in mammalian cells, primers were configured so that the forward oligonucleotide supplied the upstream homology stretch of pEGFP-C1 plus a BglII cleavage motif, and the reverse oligonucleotide contributed the downstream homology stretch of pEGFP-C1 plus a SalI cleavage motif. Following amplification, the DNA product was simultaneously cut with BglII (Thermo Fisher Scientific, FD0084) and SalI (Thermo Fisher Scientific, FD0644) and then integrated via homology-directed joining into the pEGFP-C1 backbone that had been linearized by the same two restriction enzymes. A parallel cloning approach was taken for PVC cargo construction: forward primers incorporated the upstream homology arm of pBBRN-pdp1N50 and a BamHI site, whereas reverse primers appended the downstream homology arm of pBBRN-pdp1N50 and a HindIII site. The resulting PCR product, once doubly cleaved with BamHI (Thermo Fisher Scientific, FD0054) and HindIII (Thermo Fisher Scientific, FD0505), was recombined into the pBBRN-pdp1N50 acceptor plasmid that had undergone the same dual digestion, enabling subsequent protein manufacture and PVC encapsulation. Similarly, the chemically synthesized fragment, after BamHI/HindIII double digestion, was inserted into pMV261, which had been opened with the matching enzymes, thus permitting protein production in M. smegmatis.

### *Immunoblot detection workflow*

Aliquots of PVC-containing protein solutions and HEK293T whole-cell lysates prepared for Western blotting were combined with reducing sample buffer and heated to 99 °C for 10 min. In contrast, *M. smegmatis* pellets collected from cellular infection experiments were mixed with sample buffer and heated at 99 °C for 1 hour. The denatured protein mixtures were then fractionated on 12% tris-glycine SDS-PAGE gels. Resolved polypeptides were subsequently electrotransferred onto PVDF membrane sheets (Millipore, Burlington, MA, USA, IPVH00010) via a Bio-Rad wet transfer module. After transfer, the membranes were saturated with 5% bovine serum albumin diluted in TBST for 1 h, then probed with the designated primary antibody overnight at 4 °C. When necessary, a secondary incubation step was performed using horseradish peroxidase-conjugated anti-rabbit or anti-mouse immunoglobulin reagents. Bound antibodies were visualized by applying chemiluminescent detection reagents (NCM Biotec, Suzhou, China, P10060), and the resulting luminescent signals were digitally acquired on an imaging platform (Tanon, Shanghai, China, 5200Multi). The collection of primary immunological probes employed in these experiments comprised: anti-Flag (Sigma-Aldrich, St. Louis, MI, USA, F3165), anti-p-RIP (Cell Signaling, Danvers, MA, USA, 65746), anti-HSP65 (Santa Cruz, TX, USA, sc-58170), anti-GFP (Huaxingbio, Beijing, China, HX1824), anti-His (Huaxingbio, HX1822), and anti-GAPDH-HRP (Bioworld, St. Louis Park, MN, USA, MB001H). The antiserum recognizing Pvc16 was raised in rabbits immunized with bespoke synthetic peptide antigens (Genscript, Piscataway, NJ, USA).

### *Isolation and enrichment of PVC particles*

The procedure for PVC preparation was carried out following the methodology detailed in our earlier report [18]. In outline, the LysR-encoding plasmid pBR322 was introduced into *E. coli* EPI300 cells already carrying the plasmid pRK404-PVC, which directs the synthesis of the PVC structural components. In experiments requiring the incorporation of cargo proteins, a third plasmid, pBBRN-pdp1N50, harboring the gene of interest, was co-transformed with the identical host background. Liquid cultures were propagated in 200 mL of LB broth at 30 °C for 16 h. The bacterial biomass was collected and taken up in 30 mL of chilled lysis buffer P [composed of 25 mM Tris-HCl (pH 7.4), 140 mM NaCl, 3 mM KCl, plus deoxyribonuclease I at 50 μg/mL, lysozyme at 200 μg/mL, 0.5% Triton X-100, 5 mM MgCl2, and a 1× protease inhibitor mixture (MedChemExpress, HY-K0010)]. The resulting slurry was warmed to 37 °C for a half-hour incubation to drive cellular disruption. After lysis, insoluble debris was eliminated by spinning at 14,000 rpm for 10 min at ambient temperature. The cleared lysate was then transferred to ultracentrifugation tubes and spun at 150,000× g for 60 min at 4 °C to sediment macromolecular assemblies. The ultracentrifugation pellet was delicately resuspended in 1 mL of sterile phosphate-buffered saline (PBS). A subsequent clarifying spin at 14,000 rpm for 10 min at 4 °C was performed to discard any remaining particulate contamination. The resulting supernatant was subjected to an additional round of ultracentrifugation under identical conditions (150,000× g, 60 min, 4 °C) to further refine the PVC preparation. Ultimately, the enriched pellet was taken up in 200 μL of ice-cold PBS and polished by a final centrifugation step at 14,000 rpm for 10 min at 4 °C. The supernatant, now containing highly purified PVC particles, was divided into single-use aliquots and kept at 4 °C until needed.

### *Transient transfection of mammalian cells*

Upon attaining approximately 70% monolayer confluency, HEK293T cultures were transiently transfected with the constructs pEGFP-C1, pEGFPC1-MmTG, pEGFPC1-C159S, and pEGFPC1-MAB 4306 at

a DNA dosage of 0.1 μg per well (for 96-well formats) or 0.5 μg per well (for 24-well formats) using the PolyJet transfection reagent (SignaGen, Frederick, MD, USA, SL100688) in strict accordance with the protocol supplied by the vendor. Transgene expression efficiency was evaluated 24 h post-transfection by monitoring GFP-derived fluorescence through an inverted fluorescence microscope, after which downstream assays were initiated.

### *Measurement of cellular viability*

Quantitative assessment of cell viability was performed using the Cell Counting Kit-8 (MedChemExpress, HY-K0301) and the CellTiter-Lumi™ Luminescent Cell Viability Assay Kit (Beyotime, Shanghai, China, C0065M), both performed exactly as specified in the accompanying product literature. Each assay condition included at least 3 replicate wells, and each experimental run was independently repeated at least 3 times.

### *Macrophage challenge with engineered M. smegmatis*

J774A.1 and THP-1 cells were dispensed into 96-well culture plates at a density of $1 \times 10^5$ cells per well and maintained in medium devoid of antibiotics before infection. The monolayer cultures were subsequently exposed to Ms_Vec and Ms_MmTG at a multiplicity of infection (MOI) of either 5 or 10. Following a 4-hour bacterial challenge period, the cell layers were rinsed with PBS, after which extracellular bacteria were eliminated by treatment with gentamicin at 100 μg/mL for an additional 4-hour interval. The cells were then washed once more with PBS and cultured for an additional 18 h in antibiotic-free medium. Cellular morphology was examined by light microscopy, and viability was subsequently quantified.

### *Computational analyses and statistical methods*

All nucleotide and amino acid sequences were retrieved from the NCBI and UniProt databases. Multiple sequence alignments and phylogenetic tree generation were performed using DNAMAN and MEGA12. Tree rendering for publication purposes was carried out with FigTree version 1.4.4. Three-dimensional protein structure predictions were computed using the AlphaFold3.0 platform, and molecular visualization and structural superimpositions were performed in PyMOL. Numerical data were processed and graphed using GraphPad Prism, with statistical significance evaluated by two-tailed Student's t-test and analysis of variance (ANOVA) where appropriate.

## Results and Discussion

### *MmTG suppresses cellular proliferation*

We first generated the eukaryotic expression construct pEGFP-C1-MmTG for MmTG and carried out transient expression in HEK293T cells. Western blotting verified the production of both GFP and the GFP-MmTG chimeric proteins **(Figure 1a)**. At 24 and 48 hours after GFP-MmTG expression, marked differences in cellular viability were observed compared with the control condition **(Figure 1b)**. Given that ATP serves as the primary energy currency of cells and is closely linked to cell viability, we evaluated cell health by measuring ATP. The findings indicated that transient production of the MmTG protein induced toxic effects in HEK293T cells, suggesting it may function as a cytotoxic effector molecule of M. microti.

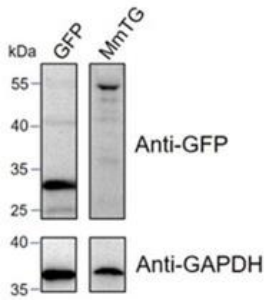


a)

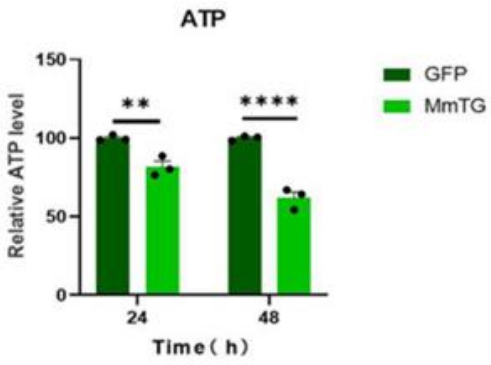


b)

**Figure 1.** The MmTG protein from *M. microti* exhibits cytotoxic properties: (a) Western blotting was used to verify the transient expression of MmTG in HEK293T cells. GAPDH was used as a loading control. Lanes from the identical blot were reordered. (b) HEK293T cell viability was determined through ATP level quantification at 24 h and 48 h after transient MmTG expression. (**) $P < 0.01$; (****) $P < 0.0001$.

### *M. smegmatis-based infection experiments*

To delve deeper into the noxious effects of MmTG, we established *M. smegmatis* infection models in macrophage cell lines and subsequently assessed cellular viability using a Cell Counting Kit-8 (CCK-8) assay. As presented in **Figure 2a**, we achieved robust heterologous production of MmTG within *M. smegmatis*. Exposing J774A.1 and THP-1 macrophages to the genetically modified *M. smegmatis* strain for a period of 24 h resulted in a substantial impairment of cell viability **(Figure 2b)**, with

human-derived THP-1 cells exhibiting an even greater sensitivity.

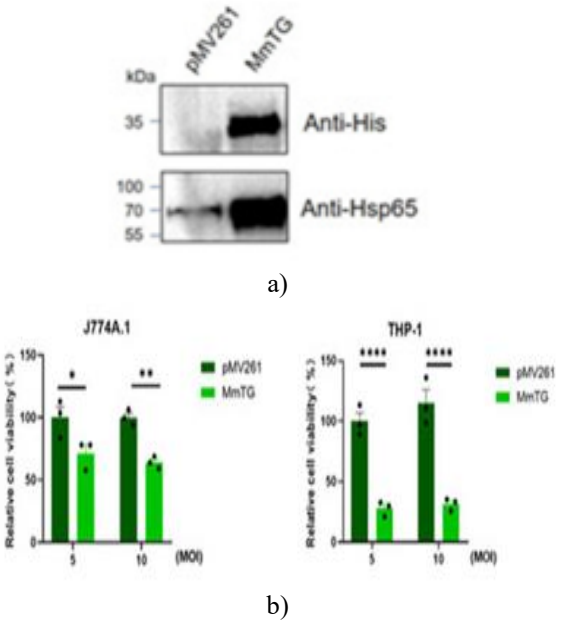


**Figure 2.** Eukaryotic macrophage challenge with *M. smegmatis* harboring MmTG: (a) Recombinant MmTG was produced in M. smegmatis, and its presence was verified by immunoblotting. Total protein extracts from *M. smegmatis* engineered to express MmTG were resolved and probed with an anti-His antibody to ascertain the production of His-tagged MmTG. The empty pMV261 plasmid was employed as a negative control. Detection of Hsp65 served as a loading reference. (b) The viability of J774A.1 and THP-1 macrophages was quantified through CCK-8 measurement 24 h post-challenge with *M. smegmatis* producing MmTG. (*) $P < 0.05$; (**) $P < 0.01$; (****) $P < 0.0001$.

## *Cys159 is indispensable for activity*

The catalytic triad composed of Cys-His-Asp is strongly conserved across TGases, with particular importance attached to Cys159, which occupies a critical position in both evolutionary lineage and enzymatic function **(Figure 3a)**. Furthermore, in silico structural modeling of MmTG using AlphaFold3 resolved its three-dimensional organization: four α-helical segments and two β-sheet strands linked by intervening loop structures **(Figure 3b)**, displaying a striking resemblance to established transglutaminase architectural motifs. We carried out site-directed mutagenesis to introduce the C159S substitution and transiently expressed the mutant construct in HEK293T cells. Viability measurements revealed that the cytotoxic effect of the mutant on eukaryotic cells was sharply reduced compared with that of the unmodified protein **(Figure 3c)**. A clear divergence in cellular appearance between cultures receiving the mutant versus the wild-type construct was evident at both evaluated intervals **(Figure 3d)**.

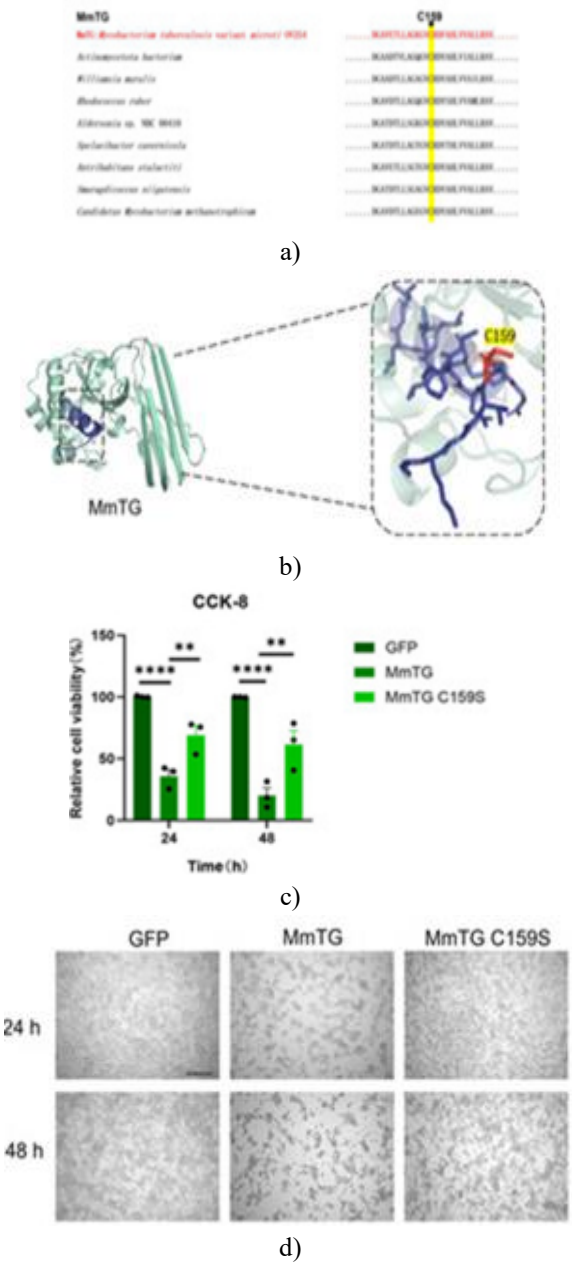


**Figure 3.** The active-site cysteine of MmTG is highly conserved and required for MmTG-mediated cytotoxicity: (a) The C159 residue within the active center of MmTG exhibited strict conservation across diverse genera. (b) Three-dimensional structural representation of the MmTG module. The MmTG sequence was subjected to AlphaFold3-based modeling, and the critical C159 side chain was marked. (c) HEK293T cell viability was evaluated through CCK-8 assay at 24 h and 48 h following transient transfection with MmTG or the C159S variant. (d) Microscopic examination of HEK293T cell morphology 24 h and 48 h after transient expression of either MmTG or C159S. Scale bars, 200 μm. (**) $P < 0.01$; (****) $P < 0.0001$.

### *MmTG is packaged into the PVC to directly eliminate murine macrophages*

To recapitulate the natural mechanism through which effector proteins are translocated into host cells via secretion apparatuses, we employed the PVC—a well-established delivery platform identified in our earlier work—to encapsulate and transport both the native and altered versions of the protein into macrophages **(Figure 4a)**, thereby confirming the functional relevance of MmTG. Mutant proteins delivered through the PVC exhibited significantly reduced toxicity, with discernible morphological alterations in the recipient cells observed at 24 h following delivery **(Figures 4b and 4c)**. These findings substantiated that MmTG operates as a cytotoxic effector of *M. microti* and that the Cys159 residue plays an indispensable part in mediating its cell-killing activity.

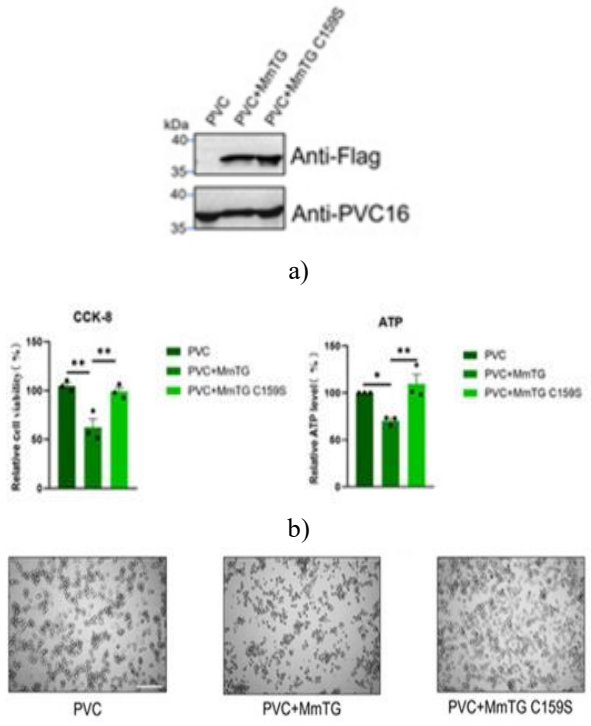


**Figure 4.** MmTG can be loaded into the PVC for direct destruction of murine macrophages: (a) Successful incorporation of MmTG was verified by Western blotting. Pvc16 served as a loading reference. (b) J774A.1 cell viability was determined via CCK-8 assay (left panel) and ATP quantification (right panel) at 24 h after PVC-mediated delivery of MmTG or the C159S variant. (c) Morphological appearance of J774A.1 cells 24 h following exposure to PVC+MmTG or PVC+MmTG C159S. Scale bars, 200 μm. (*) $P < 0.05$; (**) $P < 0.01$.

### *TGases are broadly present and elicit RIPK1 phosphorylation*

TGase enzymes are widely distributed among 1000 bacterial cells, spanning the genera *Mycobacterium*, *Nocardia*, *Gordonia*, and *Micrococcus*, with roughly three-quarters of all detected homologs clustering within *Mycobacterium* and exhibiting high sequence similarity **(Figure 5a)**. When MAB_4306, a protein homologous to MmTG in *M. abscessus*, was transiently overexpressed in HEK293T cells for 24 and 48 h, a significant impairment of cellular viability ensued **(Figure 5b)**. The PVC machinery was additionally co-opted to shuttle the homologous protein MAB_4306 into J774A.1 macrophages, where a significant loss of cell viability was also documented, and the deeply conserved Cys159 was tied to its cytotoxic properties. Furthermore, both TGase proteins were proficient at inducing RIPK1 phosphorylation, though their activation timeframes diverged—MmTG stimulated RIPK1 at the 18-hour mark, whereas MAB_4306 achieved this at 36 hours **(Figure 5c)**. Operating as a crucial intersection point for cell death signaling and inflammatory modulation, RIPK1 engagement has been established as a vital contributor to both apoptotic and necroptotic pathways, plausibly accounting for the cellular destruction observed in the present work.

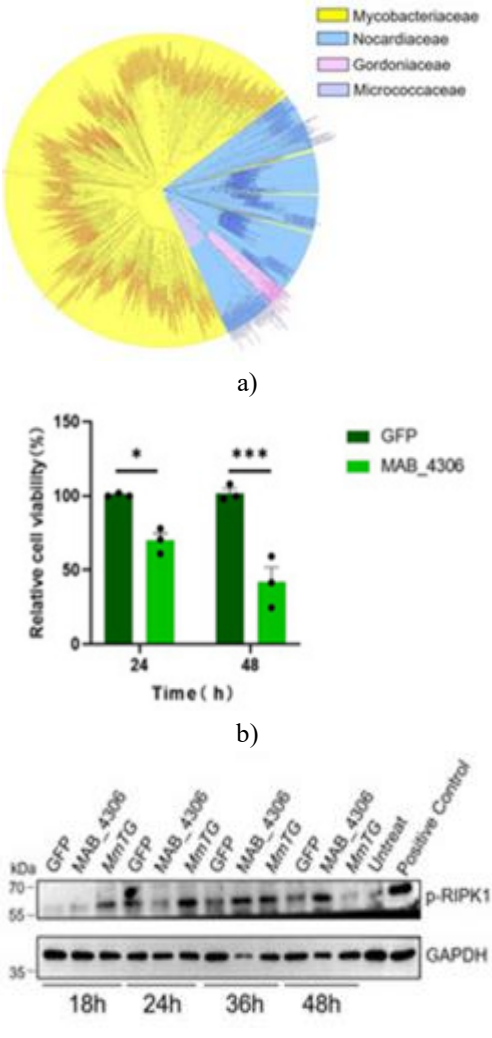


**Figure 5.** Transglutaminase is widely distributed and conserved across mycobacteria: (a) A phylogenetic tree

built using the Neighbor-Joining algorithm was constructed to interrogate the evolutionary trajectory of transglutaminase across mycobacterial lineages. (b) The viability of HEK293T cells was gauged via CCK-8 assay at the 24- and 48-hour time points after transient introduction of MAB_4306, the M. abscessus counterpart of MmTG. (c) After transfection with either MmTG or MAB_4306, the level of phosphorylated RIPK1 present in HEK293T cells was assessed through Western blot analysis. Positive control: cells were treated for 4 hours with a Necroptosis Inducer Kit containing TNF-α, SM-164, and Z-VAD-FMK. (*) $P < 0.05$; (***) $P < 0.001$.

The MTBC designates an assembly of acid-fast bacilli possessing zoonotic capabilities that generally elicit either pulmonary or extrapulmonary tuberculous disease in their hosts through single-species infection. Well-known multidrug-resistant NTM, *M. abscessus*, together with MTBC constituents such as *M. bovis* and *M. microti*, are transmissible to human populations via environmental contact, polluted water sources, undomesticated animals, agricultural livestock, or raw milk and meat derivatives [17, 19], thereby constituting a considerable hazard to communal health. Recorded human cases of *M. microti* illness have emerged predominantly in European territories [20, 21]; it is noteworthy that *M. microti* can provoke overt clinical pathology even in immunocompetent subjects [22, 23], with transmission typically arising from wildlife exposure or consumption of fecally contaminated water. Scholarly attention to *M. microti* has largely focused on epidemiological patterns [24-26], symptomatic characteristics [8], and nucleic acid-based diagnostic techniques [27-29]; conversely, probing its molecular virulence determinants or its engagement with host systems has remained sparse.

TGases are ubiquitously distributed across animals, plants, and microbes. Scientific inquiry into mTGs has been weighted toward three-dimensional structure determination, recombinant overproduction and downstream purification methodologies, and deployment in industrial-scale food bioprocessing. Yet, the mechanistic underpinnings of their interactions with eukaryotic hosts in pathogenic contexts have remained elusive. The investigation described herein furnishes the first body of evidence intimating that TGase may fulfill an integral function in mycobacterial pathogenesis by orchestrating cytotoxicity via manipulation of programmed cell death circuitry. Elevated MmTG expression severely compromised the survival of HEK293T cells. Within the infected host, macrophages serve as the dominant cellular niche for M. tuberculosis and simultaneously act as pivotal immune effector cells that govern containment of bacterial proliferation [30]. To expand the characterization of MmTG-mediated cellular damage, we conducted macrophage infection trials using recombinant *M. smegmatis* and subsequently quantified the relative survival of J774A.1 and THP-1 cells. The observation that THP-1 monolayers exhibited poorer viability outcomes relative to J774A.1 cultures may be rationalized through two complementary explanations: firstly, the bacterial effector could exhibit superior receptor engagement kinetics in human-derived cells relative to those in murine cells; secondly, the divergent immunological signaling cascades mounted by distinct cell lineages upon encounter with *M. smegmatis* may differentially impinge on cell fate determinations. Earlier studies have established that THP-1 cells rely heavily on apoptotic clearance to dispose of infected cells [31-33], suggesting that this mycobacterial protein executes its cytopathic agenda by subverting apoptotic regulatory networks.

Classified as an extracellular contractile injection nanomachine, the PVC harnesses its needle-mimicking architecture to inject payload proteins (effectors) across biological membranes into susceptible host organisms [34]. Our previous studies revealed that the PVC genetic locus encodes multiple proteins with experimentally verified eukaryotic toxicity and delineated the N-terminal secretion-directing peptide sequences of these effectors (Pdp1 and Pnf). Upon translational fusion to unrelated heterologous cargoes (e.g., reporter enzymes or tumor-suppressive polypeptides), these addressing peptides were sufficient to direct the chimeric constructs to the PVC apparatus and enable their subsequent discharge into designated target cells [35]. Such observations firmly establish the PVC-based translocation platform as a uniquely enabling instrument for deconstructing the pathogenic modus operandi of the *M. microti* cytotoxic effector. MmTG was routed into J774A.1 macrophages through PVC-assisted translocation, and in agreement with the plasmid-based overexpression data, a conspicuous collapse in cell viability was recorded. The Cys-His-Asp catalytic triad embedded within TGases constitutes an indispensable determinant of biochemical reactivity. The residue Cys159 stands out as particularly consequential for the catalytic competence of MmTG, as underscored by the near-complete ablation of eukaryotic cytotoxicity observed with the C159S substitution relative to the unmodified enzyme, an outcome consistently recapitulated across both transfection and PVC-delivery experimental formats. A necessary caveat, however, arises from a prior report documenting that select mTGs naturally accumulate in the bacterial cytosol as catalytically dormant proenzymes and subsequently undergo site-specific proteolytic maturation at the bacterial envelope via self-encoded proteases. This processing event confers full enzymatic functionality [36]. Within the confines of the current study, whether the MmTG polypeptide achieves its active conformation

through a comparable zymogen-to-active-enzyme transition has not been determined. This unresolved issue remains a high-priority topic for ongoing investigations.

Complementing the experimental findings, computational phylogenomic surveys disclosed that mTGs are amply represented across the mycobacterial radiation; of considerable clinical relevance, orthologous sequences were also detected in human-pathogenic species, including *M. abscessus*, *M. interjectum*, *M. marseillense*, *M. parmense*, and additional taxa. We subsequently focused on the M. abscessus counterpart, in which an analogous diminution of host cell viability was documented. The cell-killing modalities deployed by these two mTGs were assessed for their ability to trigger eukaryotic cell death. This line of inquiry brought to light that either protein possesses the ability to engage RIPK1 and provoke its hyperphosphorylation upon cell contact. RIPK1 constitutes a serine/threonine-directed protein kinase occupying a nodal intersection connecting apoptotic, necroptotic, and pro-inflammatory signal transduction axes. At the time of writing, RIPK1 has gained recognition as an attractive druggable node for therapeutic intervention in maladies such as Alzheimer's dementia, multiple sclerosis, cerebrovascular stroke, and traumatic cerebral injury [37]. That said, the fine mechanistic details governing how these two effector proteins precipitate RIPK1 phosphorylation, the precise modalities of cell death subsequently engaged, and the potential participation of auxiliary protein-binding partners or small-molecule cofactors in the lethal cascade remain inadequately defined and require rigorous future validation.

## Conclusion

The present investigation demonstrates that MmTG exhibits pronounced cytotoxicity against eukaryotic host cells. The residue Cys159 constitutes a conserved catalytic center whose substitution via site-directed mutagenesis profoundly diminishes this toxic potential. Computational surveys indicate that TGase enzymes enjoy broad phylogenetic representation and strong sequence conservation across the genus *Mycobacterium*. Experimental evidence shows that both MmTG and its structural homolog can trigger RIPK1 phosphorylation, suggesting that this widely conserved mycobacterial TGase family may operate through shared cytotoxic mechanisms. Collectively, these observations provide a valuable foundation for future exploration of mycobacterial pathogenic strategies.

**Acknowledgments:** We thank all members of the investigator's lab for helpful discussions and the Core Facilities and Service Centers at NIPB and CAMS&PUMC for assistance with ultracentrifugation.

**Conflict of interest:** None

**Financial support:** This work was supported by the National Key R&D Program of China (2023YFE0113400), the Beijing Natural Science Foundation (5244051 and L248066), the CAMS Innovation Fund for Medical Sciences (2021-I2M-1-037 and 2023-I2M-2-001), the Special Research Fund for Central Universities, Peking Union Medical College (3332024177 and 3332023055), and the Non-profit Central Research Institute Fund of Chinese Academy of Medical Sciences (2023-PT310-04).

**Ethics statement:** None

## References

1. Goletti D, Meintjes G, Andrade BB, Zumla A, Lee SS. Insights from the 2024 WHO global tuberculosis report—more comprehensive action, innovation, and investments required for achieving WHO End TB goals. Int J Infect Dis. 2025;150:107325.
2. Nieto Ramirez LM, Mehaffy C, Dobos KM. Systematic review of innate immune responses against Mycobacterium tuberculosis complex infection in animal models. Front Immunol. 2024;15:1467016.
3. Helaine S, Conlon BP, Davis KM, Russell DG. Host stress drives tolerance and persistence: the bane of antimicrobial therapeutics. Cell Host Microbe. 2024;32(6):852-62.
4. Liebenberg D, Gordhan BG, Kana BD. Drug resistant tuberculosis: implications for transmission, diagnosis, and disease management. Front Cell Infect Microbiol. 2022;12:943545.
5. Cappelluti MA, Poeta VM, Valsoni S, Quarato P, Merlin S, Merelli I, et al. Durable and efficient gene silencing in vivo by hit-and-run epigenome editing. Nature. 2024;627(8003):416-23.
6. Esteban J, Munoz-Egea MC. Mycobacterium bovis and other uncommon members of the Mycobacterium tuberculosis complex. Microbiol Spectr. 2016;4(6).
7. van Soolingen D, van der Zanden AG, de Haas PE, Noordhoek GT, Kiers A, Foudraine NA, et al. Diagnosis of Mycobacterium microti infections among humans by using novel genetic markers. J Clin Microbiol. 1998;36(7):1840-5.
8. Peterhans S, Landolt P, Friedel U, Oberhansli F, Dennler M, Willi B, et al. Mycobacterium microti: not just a coincidental pathogen for cats. Front Vet Sci. 2020;7:590037.
9. Pym AS, Brodin P, Brosch R, Huerre M, Cole ST. Loss of RD1 contributed to the attenuation of the live tuberculosis vaccines Mycobacterium bovis BCG and

Mycobacterium microti. Mol Microbiol. 2002;46(3):709-17.
10. Cavanagh R, Begon M, Bennett M, Ergon T, Graham IM, de Haas PE, et al. Mycobacterium microti infection (vole tuberculosis) in wild rodent populations. J Clin Microbiol. 2002;40(9):3281-5.
11. Anami Y, Tsuchikama K. Transglutaminase-mediated conjugations. Methods Mol Biol. 2020;2078:71-82.
12. Kieliszek M, Misiewicz A. Microbial transglutaminase and its application in the food industry. A review. Folia Microbiol (Praha). 2014;59(3):241-50.
13. Sarkar NK, Clarke DD, Waelsch H. An enzymically catalyzed incorporation of amines into proteins. Biochim Biophys Acta. 1957;25(2):451-2.
14. Lerner A, Benzvi C, Vojdani A. The frequently used industrial food process additive, microbial transglutaminase: boon or bane. Nutr Rev. 2025;83(4):e1286-94.
15. Jiang F, Li N, Wang X, Cheng J, Huang Y, Yang Y, et al. Cryo-EM structure and assembly of an extracellular contractile injection system. Cell. 2019;177(2):370-83.
16. Wang X, Shen J, Jiang F, Jin Q. The Photorhabdus virulence cassettes RRSP-like effector interacts with cyclin-dependent kinase 1 and causes mitotic defects in mammalian cells. Front Microbiol. 2020;11:366.
17. Huard RC, Lazzarini LC, Butler WR, van Soolingen D, Ho JL. PCR-based method to differentiate the subspecies of the Mycobacterium tuberculosis complex on the basis of genomic deletions. J Clin Microbiol. 2003;41(4):1637-50.
18. Wang Y, Zhang X, Feng X, Wang X, Jin Q, Jiang F. Purification of Photorhabdus virulence cassette (PVC) protein complexes from Escherichia coli for artificial translocation of heterologous cargo proteins. Bio Protoc. 2024;14(2):e4966.
19. Chakaya J, Khan M, Ntoumi F, Aklillu E, Fatima R, Mwaba P, et al. Global tuberculosis report 2020—reflections on the global TB burden, treatment and prevention efforts. Int J Infect Dis. 2021;113(Suppl 1):S7-S12.
20. de Jong E, Rentenaar RJ, van Pelt R, de Lange W, Schreurs W, van Soolingen D, et al. Two cases of Mycobacterium microti-induced culture-negative tuberculosis. J Clin Microbiol. 2009;47(9):3038-40.
21. van de Weg CAM, de Steenwinkel JEM, Miedema JR, Bakker M, van Ingen J, Hoefsloot W. The tough process of unmasking the slow-growing mycobacterium: case report of Mycobacterium microti infection. Access Microbiol. 2020;2(3):acmi000074.
22. Foudraine NA, van Soolingen D, Noordhoek GT, Reiss P. Pulmonary tuberculosis due to Mycobacterium microti in a human immunodeficiency virus-infected patient. Clin Infect Dis. 1998;27(6):1543-4.
23. Niemann S, Richter E, Dalugge-Tamm H, Schlesinger H, Graupner D, Konigstein B, et al. Two cases of Mycobacterium microti-derived tuberculosis in HIV-negative immunocompetent patients. Emerg Infect Dis. 2000;6(5):539-42.
24. Michelet L, Richomme C, Reveillaud E, De Cruz K, Moyen JL, Boschiroli ML. Mycobacterium microti infection in red foxes in France. Microorganisms. 2021;9(6):1257.
25. Nikolayevskyy V, Kranzer K, Niemann S, Drobniewski F. Whole genome sequencing of Mycobacterium tuberculosis for detection of recent transmission and tracing outbreaks: a systematic review. Tuberculosis (Edinb). 2016;98:77-85.
26. Perez de Val B, Sanz A, Soler M, Allepuz A, Michelet L, Boschiroli ML, et al. Mycobacterium microti infection in free-ranging wild boar, Spain, 2017-2019. Emerg Infect Dis. 2019;25(11):2152-4.
27. Smith NH, Crawshaw T, Parry J, Birtles RJ. Mycobacterium microti: more diverse than previously thought. J Clin Microbiol. 2009;47(8):2551-9.
28. Orgeur M, Frigui W, Pawlik A, Clark S, Williams A, Ates LS, et al. Pathogenomic analyses of Mycobacterium microti, an ESX-1-deleted member of the Mycobacterium tuberculosis complex causing disease in various hosts. Microb Genom. 2021;7(2):000505.
29. Moens C, Bogaerts B, Lorente-Leal V, Vanneste K, De Keersmaecker SCJ, Roosens NHC, et al. Genomic comparison between Mycobacterium bovis and Mycobacterium microti and in silico analysis of peptide-based biomarkers for serodiagnosis. Front Vet Sci. 2024;11:1446930.
30. Russell DG, Simwela NV, Mattila JT, Flynn J, Mwandumba HC, Pisu D. How macrophage heterogeneity affects tuberculosis disease and therapy. Nat Rev Immunol. 2025;25(6):370-84.
31. Chen C, Lin H, Karanes C, Pettit GR, Chen BD. Human THP-1 monocytic leukemic cells induced to undergo monocytic differentiation by bryostatin 1 are refractory to proteasome inhibitor-induced apoptosis. Cancer Res. 2000;60(16):4377-85.
32. Ren Y, You X, Zhu R, Li D, Wang C, He Z, et al. Mutation of Pseudomonas aeruginosa LasI/RhlI diminishes its cytotoxicity, oxidative stress, inflammation, and apoptosis on THP-1 macrophages. Microbiol Spectr. 2024;12(1):e0414623.
33. Zhu H, Dinsdale D, Alnemri ES, Cohen GM. Apoptosis in human monocytic THP-1 cells involves several distinct targets of N-tosyl-L-phenylalanyl chloromethyl ketone (TPCK). Cell Death Differ. 1997;4(7):590-9.

34. Green ER, Mecsas J. Bacterial secretion systems: an overview. Microbiol Spectr. 2016;4(1).
35. Jiang F, Shen J, Cheng J, Wang X, Yang J, Li N, et al. N-terminal signal peptides facilitate the engineering of PVC complex as a potent protein delivery system. Sci Adv. 2022;8(17):eabm2343.
36. Pasternack R, Dorsch S, Otterbach JT, Robenek IR, Wolf S, Fuchsbauer HL. Bacterial pro-transglutaminase from Streptoverticillium mobaraense—purification, characterisation and sequence of the zymogen. Eur J Biochem. 1998;257(3):570-6.
37. Degterev A, Ofengeim D, Yuan J. Targeting RIPK1 for the treatment of human diseases. Proc Natl Acad Sci U S A. 2019;116(20):9714-22.